

# Adaptive Predictive Control for Torque Applying System of High-powered Test Rig

Aida Parvaresh<sup>1,2</sup>, Mohsen Mardani<sup>2</sup>

<sup>1</sup>K.N Toosi University of Technology, Tehran, Iran

<sup>2</sup>Sharif University of Technology branch of ACECR, Tehran, Iran

e-mail: Mardani@acecr.ac.ir

## Abstract

This paper proposes the implementation of a novel predictive control scheme known as adaptive generalized predictive control (AGPC) in the actuation system of a high-powered test rig. Through the use of actuation system, the required torque for simulating different conditions can be applied to the tested gearboxes. The accurate and precise control of this system is of great importance as it affects the overall performance of the test rig. The considered actuation system in this investigation is electro-hydraulically driven with nonlinear and uncertain characteristics. The performance of the proposed control scheme in different conditions of the parametric uncertainty as well as presence of disturbances are evaluated and the results are discussed. The results confirmed the superior performance of the proposed scheme in different studied conditions.

**Keywords:** mechanically closed-loop test rig, Predictive control, Torque applying system, Adaptive control, Parameterized identification

Nomenclature			
$A, B, C$	System polynomials	$t_s$	Sampling time
$E(j), F(j)$	Polynomials of Diophantine equation	$u(k)$	System input
$J$	Cost function	$v$	Control horizon
$S_{exc}$	Excitation signal	$y(k)$	System Output
$TF$	Transfer function	$z^{-1}$	One-step backward operator
$W_{des}$	Desired reference	$\omega_i$	Frequency of excitation signals
$k$	Discrete time sample	$\varphi(t)$	Regression vector
$l$	Number of sine signal	$\lambda(j)$	Control weighting coefficient
$n$	System order	$\xi(k)$	Uncorrelated random noise with zero mean
$na, nb, nc$	Degrees of polynomials $A, B, C$	$\theta$	Vector of unknown parameters
$p$	Prediction horizon	$\Delta$	Difference operator
$s_i$	Amplitude of excitation signals		

## 1. Introduction

According to the importance of evaluating the high-powered gearboxes that are widely used in helicopters, test rigs are developed. By checking the overall performance through the use of test rigs, the occurrence of major failures would be minimized [1]. The test rigs are capable of providing realistic conditions that are mostly encountered during the performance with the help of varying the applied torque and speed of the system [2]. Hence, an actuation system is required for the implementation of desired torque automatically. Among the different systems used for actuating, electro-hydraulically-powered systems are of great importance considering their superior characteristics. These characteristics include higher power/force generation, lower size of equipment, fast response, improved robustness and good positioning accuracy [3], [4] and [5]. However, these actuators suffer from the existing nonlinearities and time-dependent characteristics, which would result in backlash, friction and increased complexity in modeling [6],[7]. The main issue in the use of these systems for the efficient control of actuation systems is to achieve enhanced accuracy besides maintaining robustness.

Prior to the design of controller, an appropriate modeling of electro hydraulic actuator (EHA) is very important concerning its influences on the performance of designed controller. Different approaches have been used for modeling these actuators, among which, it can be mentioned to linearized mathematical models, simplified physical models as well as data-driven models. Considering the nonlinear and uncertain dynamics of EHA, the use of data-driven modeling is superior compared to other approach [8], [9] and [10]. Yao et al. [11] utilized the dynamic model of EHA in the form of mathematical relations and also used multi-layered neural network (NN) structure as a black-box estimator to overcome the mismatched and matched disturbances besides improving the compensation accuracy. In fact, the whole system was not identified and only the disturbances were supposed to be identified. They declared the excellent performance of the proposed strategy for the estimation of existing uncertainties in the system. Lu et al. [7], used a hybrid online/offline identification for the model parameters of hydraulic system, including time-varying and nonlinear deformation forces. They obtained the dynamic model of the system regarding the pressure, displacement, velocity and acceleration data that were obtained through conducting different experiments. The required parameters were identified by the use of nonlinear optimization algorithm, such

as the particle swarm optimization (PSO) method. Then, a tracking control strategy was implemented for the provision of satisfactory force and velocity for the piston rod to perform the desired task. Their modeling procedure and control scheme were validated through experimental tests. In the mentioned study, some parameters were estimated in an offline manner and used in the subsequent online identification step, which increased the computational cost and also in addition, the whole dynamics of the system was not identified.

After achieving an appropriate model for the system, the control issue can be addressed. Several investigations have been dedicated to the development of control scheme for precise position control of EHA with the usage in the industrial applications. Takloo et al. [12] used fractional-order proportional-integral-derivative (FOPID) controller with a mathematical model of EHA system to control the actuation system in a mechanically closed-loop test rig constructed for testing the gearboxes. They declared the improved accuracy and increased speed in comparison with conventional PID controllers. In another research, Maddahi et al. [13] used the same controller for the position control of hydraulic actuators with unknown parameters. The parameters were determined through system identification (SI) procedure. In addition, the controller parameters were tuned experimentally with an iterative algorithm to achieve the tracking accuracy as well as stability. In a research by Li et al. [14], a nonlinear back-stepping controller was developed for high velocity tracking performance and achieving reduced energy consumption. In addition, radial-based function neural-network (RBFNN) was utilized to compensate the uncertainties and disturbances in the velocity control loop. In this study, the system model was obtained in the state-space form and only the load force was estimated.

The optimal control approach to achieve energy efficiency and force tracking performance was proposed by Heybroek et al. [15] for the control of EHA. This study implemented a simplified model of the system for control purposes. In addition, a model predictive control (MPC) controller was utilized for force control; while another controller was used for energy efficiency property. The conducted study was limited to the force control rather than motion control. Rozali et al. [16] suggested the use of PID controller for controlling EHA. The model of the system was obtained through SI technique by collecting the input-output data from the real experiments and

implementation of auto-regressive models with exogenous inputs (ARX) structure. The coefficients of PID controller were tuned by Ziegler-Nichols tuning method. Their results revealed an acceptable tracking of the controller; however, the response was slow. Generally, several approaches have been proposed for the adaptive control of different systems. In [15], an output feedback control scheme was developed with the help of an unknown dynamic estimator to overcome the existing problems in previous adaptive control designs. Mostly, the traditional adaptive schemes can be classified as the designs using back-stepping or dynamic surface control or the designs using intelligent approximation-based controls such as neural networks or fuzzy logic control. The prior group requires the direct measurement of all system states. In addition, the complex implementation and stability analysis are challenging in these controllers. The latter group of controllers, despite their superior performance in the presence of uncertainties and nonlinearities, suffers from the high computational cost imposed from the tuning of several parameters. To overcome the mentioned stability issue of the prior class, a novel composite learning technique was suggested [17], which used the online recorded data together with instantaneous data to generate the prediction error. In [18], [19], a new model reference adaptive control (MRAC) framework with modified reference model was proposed to improve the transient response that was originated from the possible uncertainties in the system dynamic. In addition, the stability issue was solved by the use of a leakage term in the adaption law to guarantee the convergence.

MPC is an advanced and well-known control technique that is widely used for process control in many industrial applications [20]. This strategy implements the explicit model of the desired process to determine the control signal and predict the control variables over a certain time horizon and through the minimization of an objective function [21],[22]. This controlling approach has been utilized in different applications of EHAs [23], [24], [25] and [26]. In recent years, generalized predictive control (GPC), which is considered as a special case of MPC with its own superiorities, has gained extensive interest in various industries [27]. Through the use of this method, an equilibrium between computational cost and disturbance rejection would be obtained [28]. The problem that is mostly encountered in real applications, is the presence of disturbances and model uncertainties. According to Gao [29], both disturbances from the external environments and uncertainties induced from the un-modelled dynamics can be

included in the term disturbances. To overcome this issue, adaptive predictive control (APC) has been proposed as an efficient approach [30]. The adaptation law can be implemented through updating the parameter estimations [31]. The use of APC in different problems has led to satisfying results [32],[33]. Wang et al [34], offered the use of ultra-local MPC, which was considered as a straight-forward model-free MPC procedure. The MPC was applied to the updated linear model of the system and the requirement for the extensive data-set for training was eliminated.

In our research, after obtaining the online model of the system through the data gathered from the experimental tests, the GPC process would be used for controlling the actuation system. The highlights of this study can be summarized as follows:

- Proposing an efficient approach for simultaneous identification and control of a test rig with unknown parameters.
- Provision of adaptability as well as robustness to external disturbances and uncertain and changing dynamics.
- Reduced computational cost with the help of parameterized identification with least unknown parameters and predetermined the system structure.
- The use of parameterized control sequence calculations by piece-wise linear functions that passes the defined points in time horizon to reduce the controller computational cost.
- Achieving high accuracy tracking performance in varying conditions.

The rest of the paper is organized as follows: in Section 2, the proposed approach for the identification and control of the electro-hydraulically-driven actuation system is detailed. Section 3 is dedicated to the demonstration of experimental set-up that is supposed to be controlled. After that the obtained results are presented and discussed in Section 4. Finally, the chief findings of this study is provided in the conclusions Section.

## **2. Problem Definition**

In this study, AGPC method is used for controlling the actuation system. As mentioned, the automatic tuning of controller parameters is of great significance in industrial applications. In this scheme, updating the model parameters and regulating the coefficients are performed by an automatic tuner [35]. An optimization problem is solved at each step considering the system model and current information to find the optimum

control signal. Then, the first element of the obtained signal is applied to the system and the mentioned optimization problem is solved again using the new information [27]. The procedure is defined in the following.

Consider an unknown system, which can be changed overtime and only the input-output data are available for this system. The studied system in this paper is a single-input single-output (SISO) system, which can be described by a controller auto regression integrated moving average (CARIMA) model as follows:

$$A(z^{-1})y(k) = B(z^{-1})u(k) + C(z^{-1})\frac{\xi(k)}{\Delta} \quad (1)$$

In the above equation,  $y(k), u(k) \in \mathbb{R}$  and represent the output and input of the system, respectively. The integer  $k = 0, 1, \dots$  is the discrete time sample and  $z^{-1}$  denotes the one-step backward operator, so we define  $z^{-i}x(k) = x(k-i)$  and  $z^{-i}u(k) = u(k-i)$ . In addition,  $\xi(k)$  is also an uncorrelated random noise with zero mean that is added to the model by the operator  $\Delta = 1 - z^{-1}$ , which is a difference operator. In Eq. (1),  $A(z^{-1})$ ,  $B(z^{-1})$  and  $C(z^{-1})$  are the polynomials with the respective degrees of  $na$ ,  $nb$  and  $nc$  defined as:

$$\begin{aligned} A(z^{-1}) &= a_{na}z^{-na} + \dots + a_1z^{-1} + 1 = 1 + \sum_1^{na} a_i z^{-i} \\ B(z^{-1}) &= b_{nb}z^{-nb} + \dots + b_1z^{-1} + b_0 = \sum_1^{nb} b_i z^{-i} \\ C(z^{-1}) &= c_{nc}z^{-nc} + \dots + c_1z^{-1} + c_0 = \sum_1^{nc} c_i z^{-i} \end{aligned} \quad (2)$$

For the sake of simplicity, if white noise is considered,  $C(z^{-1}) = 1$ . So we have:

$$A(z^{-1})y(k) = B(z^{-1})u(k) + \frac{\xi(k)}{\Delta} \quad (3)$$

Here, Diophantine equation is used for deriving the past and future dynamics, which can be used for prediction purposes. In order to obtain the prediction of output  $y(k+j|k)$  at time step  $(k+j)$  through the use of available information at time  $k$ , the Diophantine equation is introduced as:

$$\begin{aligned} 1 &= E_j(z^{-1})\Delta A(z^{-1}) + z^{-j}F_j(z^{-1}) \\ \begin{cases} E_j(z^{-1}) = \sum_{i=0}^{j-1} e_{j,i}z^{-i} \\ F_j(z^{-1}) = \sum_{i=0}^{j-1} f_{j,i}z^{-i} \end{cases} \end{aligned} \quad (4)$$

In the above equation,  $E_j(z^{-1})$  and  $F_j(z^{-1})$  are the polynomial expressions. By the use of abovementioned definitions and some simplifications, the  $y(k+j|k)$  can be obtained by:

$$y(k+j|k) = E_j(z^{-1})B(z^{-1})\Delta u(k+j-1|k) + F_j(z^{-1})y(k) \quad (5)$$

The optimization problem is defined by considering a quadratic cost function as:

$$J = \sum_{j=1}^P (y(k+j|k) - W_{des}(k+j|k))^2 + \sum_{j=1}^V \lambda(j) (\Delta u(k+j-1|k))^2 \quad (6)$$

In the above equation, P and V are the prediction and control horizons, respectively. In addition,  $W_{des}$  represents the desired reference for the system. Moreover,  $\lambda(j)$  is the control weighting coefficient, which is considered as a constant value for simplicity. It is aimed to minimize the J index subjected to the existing constraints, so, we have:

$$\frac{\partial J(t)}{\partial u(t)} = 0 \quad (7)$$

The control signal increment can be obtained from:

$$\Delta U = (G^T G + \lambda I)^{-1} G^T (W - f) \quad (8)$$

In the above equation,  $f$  is a vector, which consists past inputs, past outputs and current output. In addition,  $G$  denotes the step response elements. The matrix  $G$  and  $f$  are defined as:

$$G = \begin{bmatrix} g_p & g_{p-1} & \cdots & g_{p-v+1} \\ g_{p+1} & g_p & \cdots & g_{p-v+2} \\ \vdots & \vdots & \ddots & \vdots \\ g_v & g_{v-1} & \cdots & g_{v-p+1} \end{bmatrix}, g_j = 0, \forall j \leq 0 \quad (9)$$

$$f = [f_1(k) \quad f_1(k) \quad \dots \quad f_p(k)]$$

According to the receding horizon theory, only the first element of the obtained sequence is applied to the plant,  $u(t) = u(t-1) + \Delta u(1)$ , but the equation is solved over the entire horizon of time. This would lead to the increased computational cost, which may not be fast enough to be implemented in real-time control application, especially in the case of long horizon or high inputs. To this aim, it is proposed to reduce the dimensions

of the search space by parameterizing the control sequence [36]. The idea is analogous to the curve fitting so that instead of using many discrete points, the sequence is parameterized by piece-wise linear functions that passes the defined points. With the use of this procedure, the implementation time is reduced significantly.

The possible uncertainties in the plant dynamic as well as the external or internal disturbances may affect the plant representation; i.e. the polynomials of  $A(z^{-1})$  and  $B(z^{-1})$ . The explanation represented in Equation (3) can be rewritten as follows:

$$A(z^{-1})\Delta y(k) = B(z^{-1})\Delta u(k) + \xi(k) \quad (10)$$

In the above equation, we have some known values including  $\Delta y(k)$  and  $\Delta u(k)$  and unknown values, which are the coefficients of  $A(z^{-1})$  and  $B(z^{-1})$  polynomials. The vector of unknown parameters ( $\theta$ ) and the vectors of known values ( $\phi(k)$ ) are:

$$\theta = [a_1 \quad \dots \quad a_{na} \quad b_1 \quad \dots \quad b_{nb}]$$

$$\phi(k) = \begin{bmatrix} \Delta y(k-1) & \dots & \Delta y(k-na) \\ \Delta u(k-1) & \dots & \Delta u(k-nb) \end{bmatrix} \quad (11)$$

Regarding the abovementioned definitions, Equation (10), can be stated as:

$$\Delta y(k) = \phi^T(k)\theta + \zeta(k) \quad (12)$$

Hence, in order to adapt the new conditions, the parameters should be identified and updated in an online manner. The identification procedure can be conducted through different procedures. Recursive least square (RLS) estimation is among the mostly common proposed procedures for online identification of the plants. The control scheme, which requires the online adjustment of system parameters, are often called adaptive control. One other point that should be mentioned is the order of the considered model. The order of the system can be chosen regarding the evaluation of performance besides computational cost of the different systems. This requires a multi-objective optimization, which increases the computational cost of whole procedure if it is done in each iteration.

In this research, the selection of the model was performed on the basis of Parsimony principle. This principle states the priority of selecting a model with less parameters and acceptable accuracy among the models with different orders [37]. The selection of model with less parameters would lead to less computational cost as well as the simpler design of the controller [38].



Accordingly, the order of the system is defined prior to the initiation of adaptive identification process and it is considered as a known parameter in the algorithm. The proposed algorithm is represented in Figure 1. The estimation of the parameter for the time step  $k$ , which is represented by  $\hat{\theta}(k)$  is defined by the following algorithm, which is known as RLS algorithm. For more detail about this algorithm, refer to [39]:

$$\begin{aligned}\hat{\theta}(k) &= \hat{\theta}(k+1) + L(k) \left[ y(k) - \varphi^T(k) \theta(k-1) \right] \\ L(k) &= \frac{p(k-1) \varphi(k)}{\lambda(k) + \varphi^T(k) p(k-1) \varphi(k)} \\ p(k) &= \frac{1}{\lambda(k)} \left[ p(k-1) - \frac{p(k-1) \varphi(k) \varphi^T(k) p(k-1)}{\lambda(k) + \varphi^T(k) p(k-1) \varphi(k)} \right]\end{aligned}\quad (13)$$

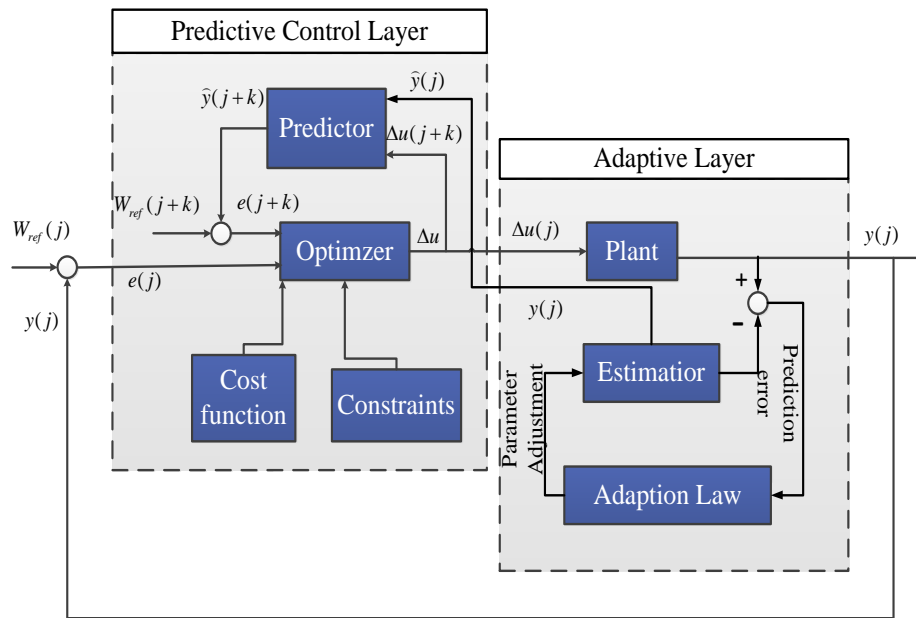


Figure 1. The proposed AGPC algorithm for the control of EHA in the actuation system of the high-powered test rig

### 3. Experimental set-up

In this paper, the torque applying system, which is a electro-hydraulically-driven system is investigated. This torque applying system is used in a closed-loop test rig, which is designed for testing the high-powered gearboxes of helicopters. The mentioned test rig was designed and fabricated in Sharif University of Technology branch of Academic Centre of Education, Culture and Research (ACECR). Low energy loss as well as provision of various torques and speeds are among the superior characteristics of the mentioned test rig. As can be seen in Figure 2, the energy in this system is circulated in a

closed-loop manner and the embedded motor is used for the compensation of energy loss as well as provision of initial power for the system start. The view of the fabricated test rig is depicted in Figure 3. For applying the required torque in the test rig to simulate the different operational conditions, EHA along with planetary gearboxes is used. The linear motion of EHA is applied on the pins as depicted in Figure 4, which transmits the motion to the rotation of the ring and the generation of required torque for the rotation of testing components. Hence, the evaluation of performance beside the fault detection would be possible by studying the system at different conditions. The characteristics of the system are provided in Table 1.

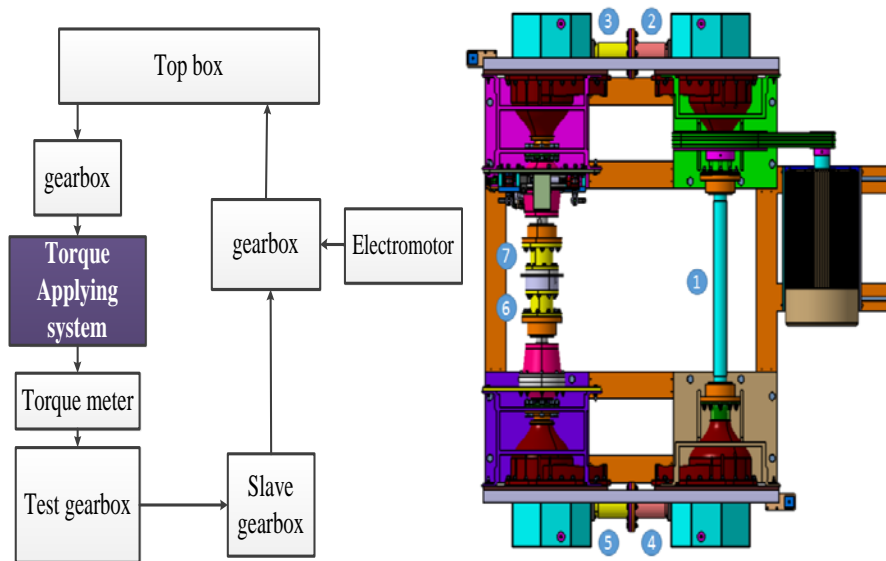


Figure 2. Schematic of the designed test rig for the high-powered test rigs

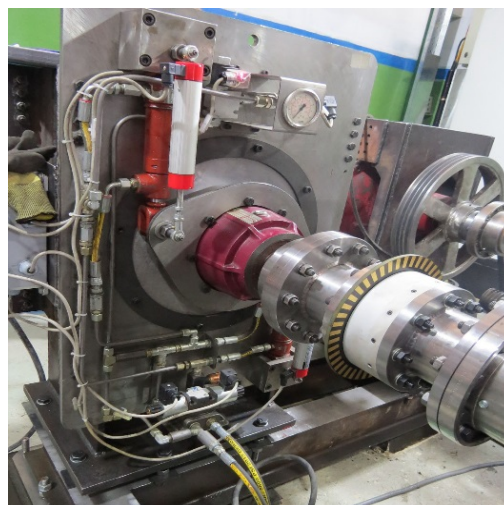


Figure 3. A view of the fabricated test rig for the high-powered gearboxes at ACECR

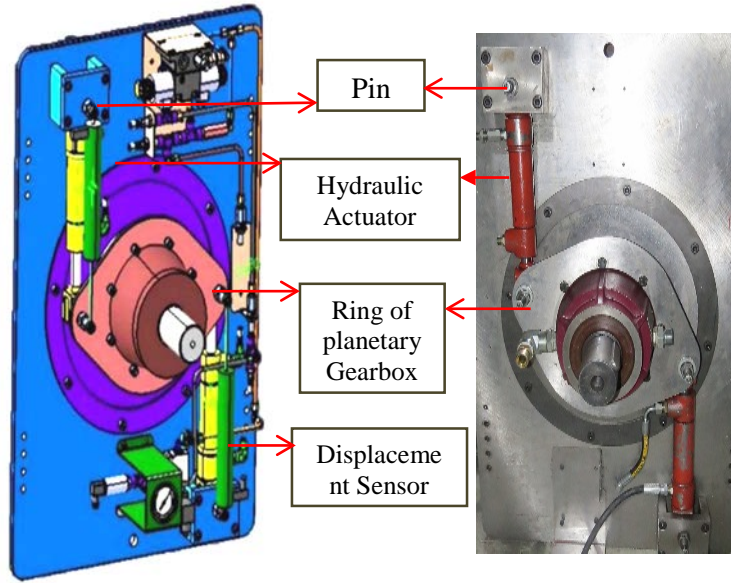


Figure 4. Real and schematic of torque applying system for actuation of high-powered test rig

Table 1. The characteristics of the test rig and the torque applying system

	specification	value
<i>Test Rig</i>	Type	Mechanically closed loop
	Max loading capacity	489 HP
	Max rotational speed	3000 rpm
<i>Torque applying system</i>	Type	Hydraulically driven
	Max hydraulic actuator course	60 mm
	Max required force	10 KN
	Force applying arm	175 mm
	Servo valve	MOOG G763004
<i>Sensor</i>	Max rotation	20 deg
	Displacement sensor	Opkon Lpc-LM 75

## 4. Results and Discussions

### 4.1. Obtaining the order of the model

In order to reduce the computational cost, the order of model should be identified prior to the control scheme. So, the model order would be a given parameter in AGPC algorithm; while the other parameters should be identified through the algorithm. To determine the appropriate order of the model, the linearized models with different orders were tested and compared in terms of accuracy and computational cost. In order to collect the required data for modeling, the input signals (voltage to the EHA) were applied to the hydraulic actuation system and the resultant outputs (displacement of EHA rod) were measured by the MOOG G763004 sensor. The applied excitation signal is illustrated as:

$$S_{exc} = \sum_{i=1}^l s_i \cos \omega_i t_s = s_1 \cos \omega_1 t_s + s_2 \cos \omega_2 t_s + \dots \quad (14)$$

In the above equation,  $S_{exc}$  represents the input signal,  $l$  is the number of sine signals to be combined and  $t_s$  denotes the sampling time. Moreover, the amplitude and frequency of the excitation signal are represented by  $s_i$  and  $\omega_i$ , respectively. The implemented system for gathering the data is depicted in Figure 5; while, the input-output data that are measured from real experiments on EHA are represented in Figure 6. In the following, the modeling of the plant is discussed.

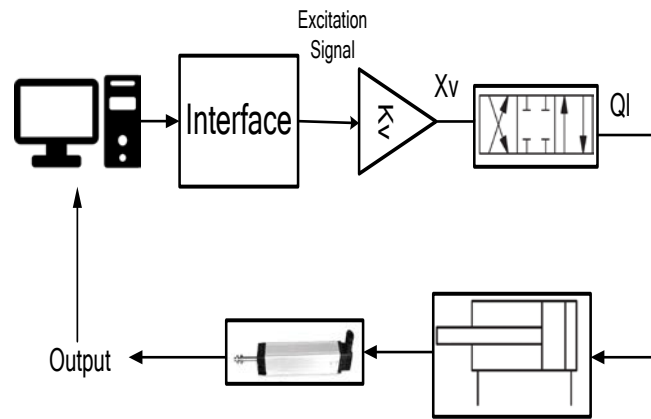


Figure 5. Data- acquisition procedure for gathering the data of torque applying system

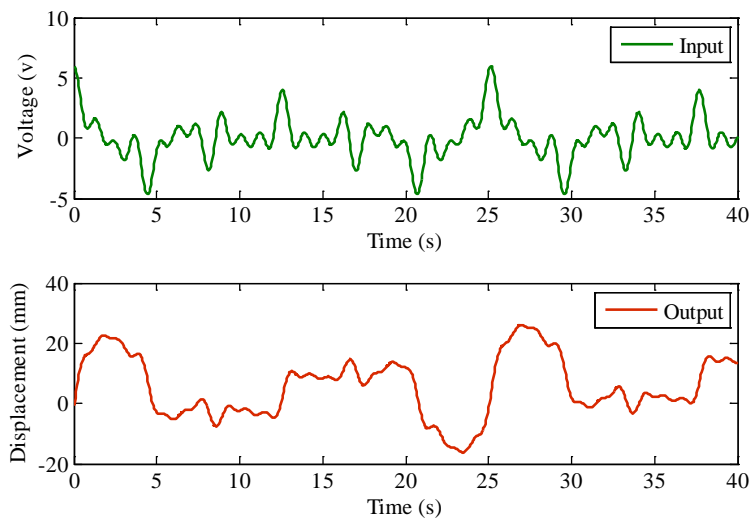


Figure 6. The gathered input-output data from the excitation of the torque applying system

In this section, structures with different orders are used to identify the system. The relationship between the inputs and outputs of the system for n-order structure can be defined as :

$$y(t) = \frac{a_{1x}z^{-1} + a_{2x}z^{-2} + \dots + a_{nx}z^{-n}}{1 - b_{1x}z^{-1} - b_{2x}z^{-2} - \dots - b_{nx}z^{-n}} u(t) \quad (15)$$

In the above equation,  $y(t)$  and  $u(t)$  are the outputs and inputs of the system, respectively, which are collected from the measurement sensors. In addition,  $z^{-n}$  represents the order of the system. Moreover,  $a_{ix}$  and  $b_{ix}$  are the unknown parameters that should be identified. The structure can be defined as:

$$\hat{y}(t | \theta) = \varphi^T(t) \cdot \theta \quad (16)$$

In this definition,  $\hat{y}(t | \theta)$  is the estimated values,  $\varphi^T(t)$  and  $\theta$  are the regressor vectors and unknown parameters vectors that are defined as follows:

$$\theta = [a_{1x} \quad a_{2x} \quad \dots \quad a_{nx} \quad b_{1x} \quad b_{2x} \quad \dots \quad b_{nx}] \quad (17)$$

$$\varphi(t) = [y(t-1) \quad \dots \quad y(t-k) \quad u(t-1) \quad \dots \quad u(t-k)] \quad (18)$$

In this paper, first-order, second-order and third-order structures were investigated. According to the results of root mean square error (RMSE) for different orders of model provided in Table 2 and outputs of the system represented in Figure 7, it can be inferred that third-order structure provides the best results. However, regarding the computational cost as another influential parameter, the second-order structure was selected. In other words, it can be stated that the model order was selected so that an acceptable compromise between the accuracy and computational cost is established. The considered model is represented as follows:

$$y_{ARX2}(t) = \frac{a_{1x}z^{-1} + a_{2x}z^{-2}}{1 + b_{1x}z^{-1} + b_{2x}z^{-2}} u(t) \quad (19)$$

Table 2. Definition of the model

Model	Parameters Vector	RSME
$y_{1\text{-order}}(t) = \frac{a_{1x}q^{-1}}{1 - b_{1x}q^{-1}} u(t)$	$\theta = [a_{1x} \quad b_{1x}]$ <b>Repressors vector</b> $\varphi(t) = [y(t-1) \quad u(t-1)]$	0.095
$y_{2\text{-order}}(t) = \frac{a_{1x}q^{-1} + a_{2x}q^{-2}}{1 - b_{1x}q^{-1} - b_{2x}q^{-2}} u(t)$	<b>Parameters Vector</b> $\theta = \begin{bmatrix} a_{1x} & a_{2x} \\ b_{1x} & b_{2x} \end{bmatrix}$	0.0253

$$y_{3\text{-order}}(t) = \frac{a_{1x}q^{-1} + a_{2x}q^{-2} + a_{3x}q^{-3}}{1 - b_{1x}q^{-1} - b_{2x}q^{-2} - b_{3x}q^{-3}}u(t)$$

**Repressors vector**

$$\varphi(t) = \begin{bmatrix} y(t-1) & u(t-1) \\ y(t-2) & u(t-2) \end{bmatrix}$$

**Parameters Vector**

$$\theta = \begin{bmatrix} a_{1x} & a_{2x} & a_{3x} \\ b_{1x} & b_{2x} & b_{3x} \end{bmatrix}$$

**Repressors vector**

$$\varphi(t) = \begin{bmatrix} y(t-1) & u(t-1) \\ y(t-2) & u(t-2) \\ y(t-3) & u(t-3) \end{bmatrix}$$

0.0178

---

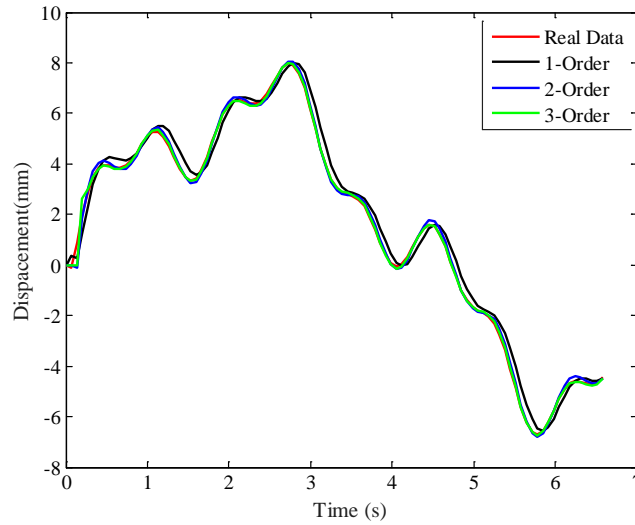


Figure 7. The comparison of the structures with different orders for predicting the system output

After selecting the model order and defining it as a known parameter in the algorithm, the controller is designed and its performance under different operational conditions is investigated in the following section.

#### 4.2. Tuning the parameters of AGPC

Tuning the AGPC parameters is of great significance considering its influence on the obtained responses. The parameters to be tuned are the lower and upper limits of prediction horizon, the control horizon, sampling time and weighting factor,  $\lambda$ . Several influential factors should be considered for the determination of these parameters. As an example, for the determination of prediction horizon, slower response of transient condition in the case of selecting higher amounts of lower limit should be noted. Moreover, the control horizon implies the freedom degree of the controller and its value should not exceeds the prediction horizon. Sampling time is also very important, which affects the accuracy and computational cost. This value is mostly restricted due to the

limitations in hardware. The weighting parameter,  $\lambda$ , affects the stability, performance and accuracy of the results. Hence, regarding these points, the considered parameters in the predictive control are as follows:

Table 3. The AGPC parameters

AGPC Parameter	Value
Prediction horizon- Upper limit	1
Prediction horizon- Lower limit	5
Control Horizon	4
Sampling time	0.001 s
$\lambda$	0.1

### 4.3. AGPC in normal conditions

For evaluating the performance of the designed controller under normal condition, the output of the system in response of varying step reference is studied and the results are depicted in Figures. 8 and 9.

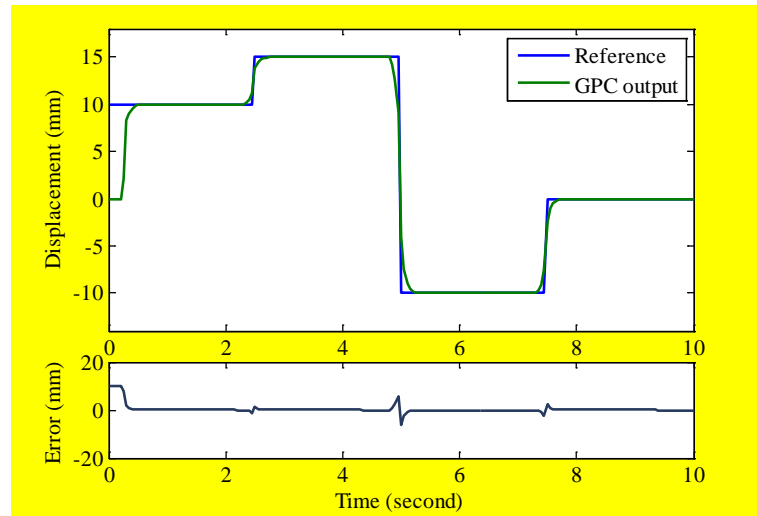


Figure 8. The performance of the proposed controller in the case of varying reference (blue line is the reference and the green line represents the GPC output) in normal condition along with the tracking error

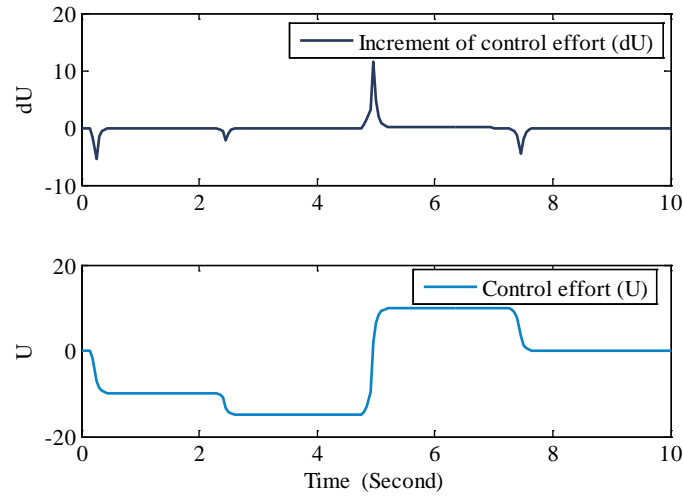


Figure 9. The increment of control effort and control effort of the proposed controller in the case of varying reference (upper diagram represents the increment of the control effort and the lower diagram indicates the control effort) in normal condition in normal condition

As can be seen Figure 8, the output of the system tracks the desired reference after about 0.6 second, without steady state error. Moreover, after varying the reference, approximately 0.2 second is required for the controller to track the new reference. Hence, the superior performance of the system in normal condition (without considering any disturbance and uncertainty) can be concluded. The increment of the control effort as well as the control effort for following the desired reference are also depicted in Figure 9.

#### 4.4. AGPC in the presence of disturbance

The performance of the designed controller is also evaluated in the presence of the external disturbances. For this purpose, a determined disturbance is applied to the system between 6<sup>th</sup> and 7<sup>th</sup> seconds as follows:

$$\text{dist} = 0.9 \times [(t > 6)(t \leq 6.5)] - 0.6 \times [(t > 6.5)(t \leq 7)]; \quad (20)$$

The performance of the actuation system in the presence of this disturbance is depicted in Figures 10 and 11. According to the results depicted in Figure 10, the controller damps the disturbance completely after 0.5 seconds. Moreover, the increment of control effort and control effort for damping the effect of disturbance are presented in Figure 11.



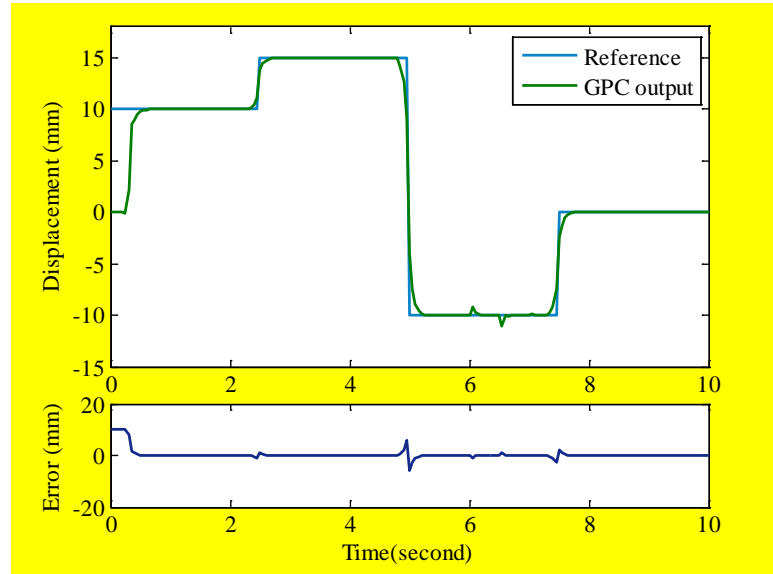


Figure 10. The performance of the proposed controller in the case of varying reference (blue line is the reference and the green line represents the system output) in the presence of disturbance along with the tracking error

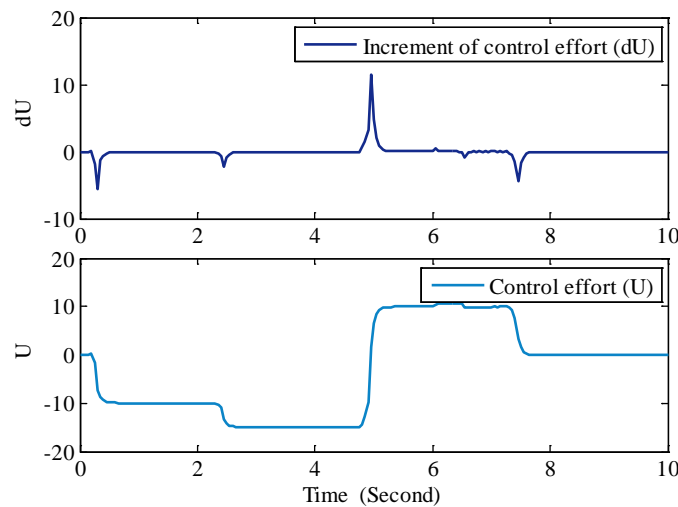


Figure 11. Increment of control effort and control effort of the proposed controller in the case of varying reference (upper diagram represents the increment of the control effort and the lower diagram indicates the control effort) in the presence of disturbance

#### 4.5. AGPC in the presence of parametric uncertainties

In this section, the performance of the system in the presence of parametric uncertainties are studied to evaluate the robustness of the proposed controller. For the

evaluation of the effect of uncertainties on the controller performance, a set of tests with different levels of uncertainties in different parameters of the plant were conducted. The considered levels of uncertainties in the parameters of the system were 10%, 15% and 30% for parameters of the plant transfer function,  $a_1$ ,  $a_2$ ,  $b_1$  and  $b_2$ . The corresponding results for  $a_1$ ,  $a_2$ ,  $b_1$  and  $b_2$  are provided in Figure 12, 13, 14 and 15, respectively. Figure 16 also represents the simultaneous uncertainties in all parameters.

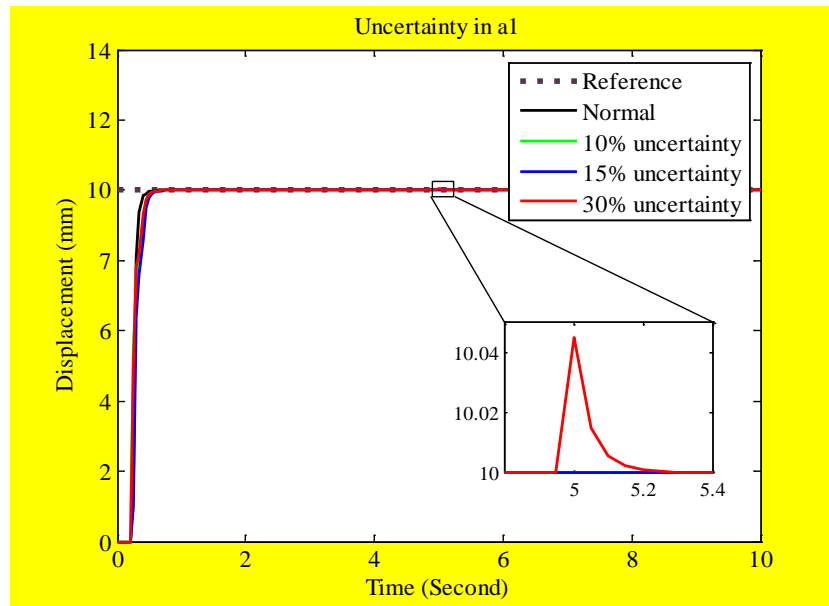


Figure 12. The performance of the proposed controller in the case of varying reference and in the presence of uncertainties in  $a_1$  parameter (Dashed line is the reference, black line is normal condition, green line represents 10% uncertainty, blue line indicates 15% uncertainty, red line shows 30% uncertainty)

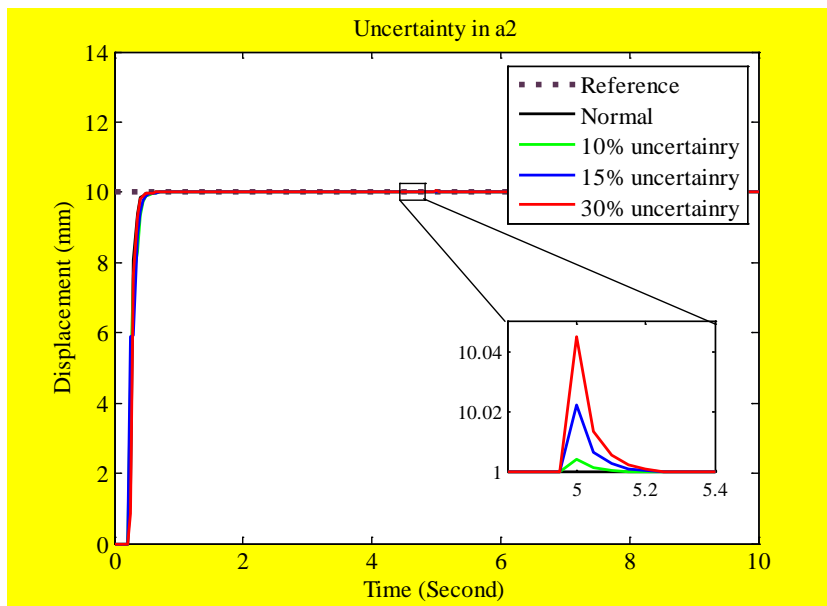


Figure 13. The performance of the proposed controller in the case of varying reference and in the presence of uncertainties in  $a_2$  parameter (Dashed line is the reference, black line is normal condition, green line represents 10% uncertainty, blue line indicates 15% uncertainty, red line shows 30% uncertainty)

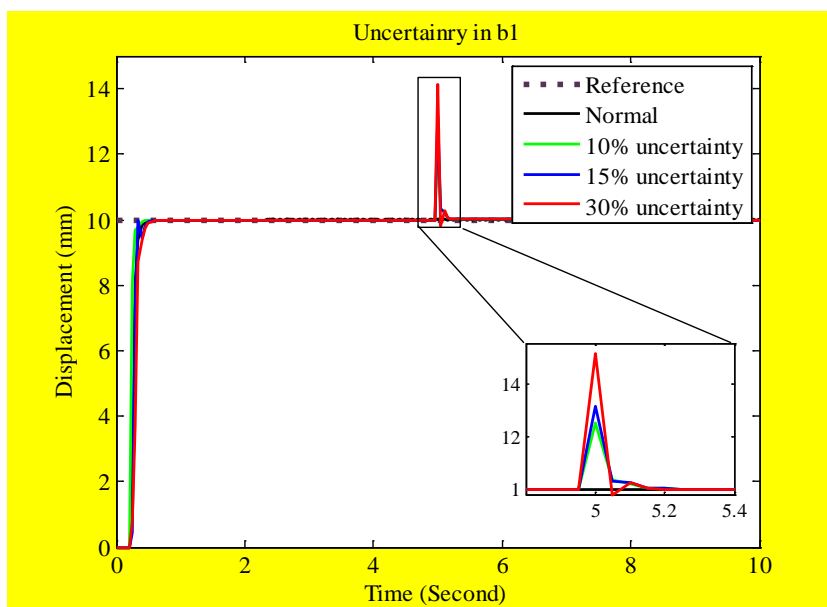


Figure 14. The performance of the proposed controller in the case of varying reference and in the presence of uncertainties in  $b_1$  parameter (Dashed line is the reference, black line is normal condition, green line represents 10% uncertainty, blue line indicates 15% uncertainty, red line shows 30% uncertainty)

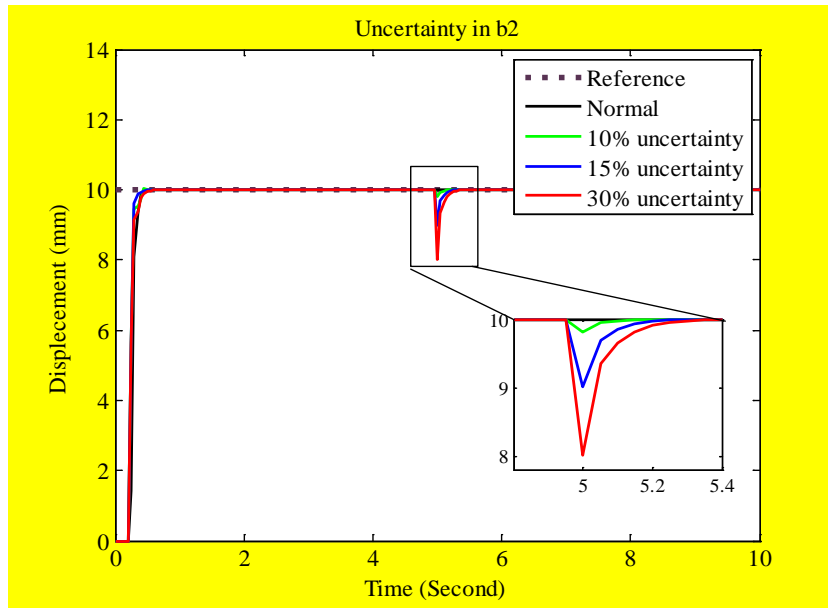


Figure 15. The performance of the proposed controller in the case of varying reference and in the presence of uncertainties in  $b_2$  parameter (Dashed line is the reference, black line normal condition, green line represents 10% uncertainty, blue line indicates 15% uncertainty, red line shows 30% uncertainty)

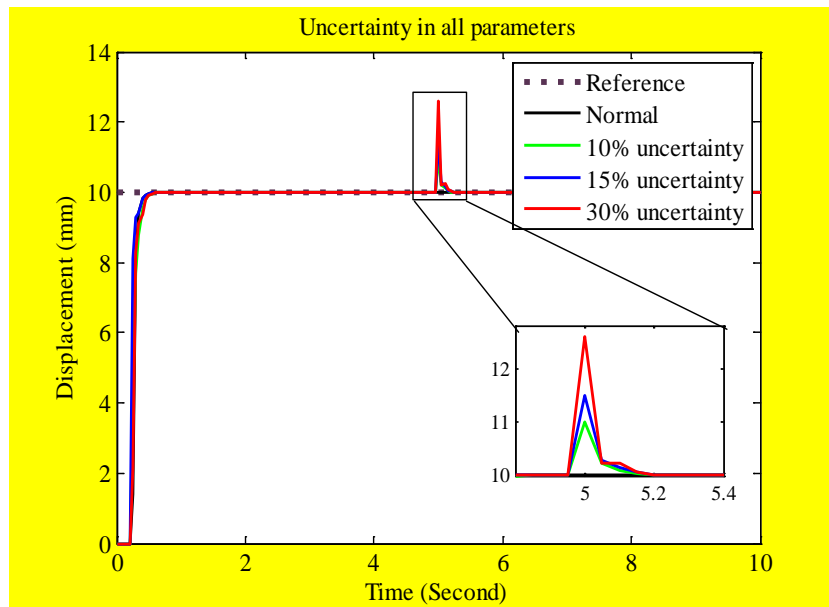


Figure 16. The performance of the proposed controller in the case of varying reference and in the presence of uncertainties in all parameter (Dashed line is the reference, black line is normal condition, green line represents 10% uncertainty, blue line indicates 15% uncertainty, red line shows 30% uncertainty)

According to the obtained results, the designed controller is capable of dealing with uncertainties in an acceptable manner. The most influential parameter from the uncertainty point of view, as can be seen in these figures, is  $b_1$  according to Figure 14.

This was expected to some extent  $b_1$  is the parameter which determines the dominant pole of the system. Then,  $b_2$  is the second influential parameters. The  $a_1$  and  $a_2$  have the least influence of the model behavior. The designed controller compensates the existed uncertainties in the first moments of performance. According to Figure 15, up to the 30% uncertainties in all parameters can be handled well by the adaptive controlling algorithm; however, the performance of the system was deteriorated in higher uncertainties in the parameters.

For better evaluation of the controller performance as well as comparison of the effect of uncertainty in different parameters, the error-based indexes, including, the root mean square error (RMSE), mean absolute error (MAE), error mean and standard deviation (Std) are evaluated. These criteria are defined as follows and the results are provided in the following Table.

$$\begin{aligned}
 RMSE &= \sqrt{(\sum_{k=1}^{n_{data}} \|y(k) - \hat{y}(k)\|_2^2) / n_d} & MAE &= \frac{1}{n_{data}} \sum_{k=1}^{n_{data}} |y(k) - \hat{y}(k)| \\
 E_{mean} &= \frac{1}{n_{data}} \sum_{k=1}^{n_{data}} (y(k) - \hat{y}(k)) & Std &= \frac{1}{n_{data}} \sqrt{\sum (y(k) - E_{mean})^2}
 \end{aligned} \tag{22}$$

In the above formulations,  $y(k)$  and  $\hat{y}(k)$  are the real and estimated values of output. In addition,  $n_{data}$  is the data size. According to the following Table, as mentioned before,  $b_1$  is the most influential parameter in uncertainty investigation. The increase in RMSE, mean, Std and MAE of this parameter is equal to 14.1, 21, 14.8 and 24.1% for 30% uncertainty compared to the normal condition.

Table. 4: The performance comparison of the uncertainties in different parameters

		Uncertainty			
		0% (normal)	10%	15%	30%
$a_1$	<i>RMSE</i>	0.1578	0.1583	0.1606	0.1663
	<i>Mean</i>	0.2510	0.2598	0.2701	0.2827
	<i>Std</i>	0.1554	0.1565	0.1587	0.1640
	<i>MAE</i>	0.2610	0.2640	0.2720	0.3130
$a_2$	<i>RMSE</i>	0.1578	0.1617	0.1631	0.17129
	<i>Mean</i>	0.2510	0.2793	0.2998	0.0310
	<i>Std</i>	0.1554	0.1591	0.1608	0.1688
	<i>MAE</i>	0.2610	0.2790	0.3001	0.312
$b_1$	<i>RMSE</i>	0.1578	0.1694	0.1767	0.1803
	<i>Mean</i>	0.2510	0.2808	0.0300	0.0311
	<i>Std</i>	0.1554	0.1679	0.1746	0.1781
	<i>MAE</i>	0.2610	0.2890	0.3380	0.0366
$b_2$	<i>RMSE</i>	0.1578	0.1607	0.1618	0.1715
	<i>Mean</i>	0.2510	0.0270	0.0278	0.2924
	<i>Std</i>	0.1554	0.1588	0.1588	0.1592
	<i>MAE</i>	0.2610	0.2780	0.2810	0.2930

## 5. Conclusion

In this paper, an adaptive case of MPC algorithm known as AGPC was used for controlling the actuation system of high-powered test rigs for gearboxes. The model of the system was obtained through the online system identification according the gathered data from the experimental tests. The precise control of the actuation system is of great importance considering the influence on the health evaluation of the gearbox. By the efficient control of the actuation system, provision of different conditions became possible. Furthermore, in order to decrease the computational cost, two schemes were utilized, parametric identification with known order and parametric calculation of the control sequence instead of calculating the control increment over the whole horizon. Different conditions were considered to evaluate the performance of the proposed control scheme, including the presence of external disturbance and parametric uncertainties. According to the obtained results, in normal conditions, the controller output tracked the reference in 0.6 s without steady state error. Moreover, approximately 0.2s was required for the controller after changing the reference for tracking. In the case with the presence of determined disturbance, the controller was able to damp the disturbance after 0.1 s completely. Furthermore, the performance of the controller in the presence of different values of uncertainties (10%, 25% and 30%) for different parameters of the transfer functions ( $a_1$ ,  $a_2$ ,  $b_1$  and  $b_2$ ) was also investigated. As the results indicated, the effect of

$b_1$  parameter was the most influential parameter among the studied parameters. However, the system can overcome the uncertainty even in the case of 30% uncertainty. Hence, the adaptability and robustness for the performance of the proposed control scheme were confirmed.

## References

- [1] L. Zhou, F. Duan, M. Corsar, F. Elasha, and D. Mba, "A study on helicopter main gearbox planetary bearing fault diagnosis," *Appl. Acoust.*, vol. 147, pp. 4–14, 2019.
- [2] P. Defreyne, S. Dereyne, K. Stockman, and E. Algoet, "An energy efficiency measurement test bench for gearboxes," *EEMODS 2013*, pp. 1–12, 2013.
- [3] N. M. Tri, D. N. C. Nam, H. G. Park, and K. K. Ahn, "Trajectory control of an electro hydraulic actuator using an iterative backstepping control scheme," *Mechatronics*, vol. 29, pp. 96–102, 2015.
- [4] W. Lee and W. K. Chung, "Disturbance-Observer-Based Compliance Control of Electro-Hydraulic Actuators With Backdrivability," *IEEE Robot. Autom. Lett.*, vol. 4, no. 2, pp. 1722–1729, 2019.
- [5] J. Huang, H. An, Y. Yang, C. Wu, Q. Wei, and H. Ma, "Model Predictive Trajectory Tracking Control of Electro-Hydraulic Actuator in Legged Robot With Multi-Scale Online Estimator," *IEEE Access*, vol. 8, pp. 95918–95933, 2020.
- [6] S. Mohammed, C. C. Soon, R. Ghazali, A. A. Yusof, Y. M. Sam, and C. M. Shern, "An Electro-Hydraulic Servo with Intelligent Control Strategy," in *MATEC Web of Conferences*, 2018, vol. 150, p. 1016.
- [7] X. Lu, Y. Bai, B. Fan, and H. Sui, "A Hybrid Offline/Online Modeling Based Tracking Control for Complex Hydraulic Driving Processes," *IEEE Access*, vol. 7, pp. 106102–106110, 2019.
- [8] A. Palermo *et al.*, "Structural coupling and non-linear effects in the experimental modal analysis of a precision gear test rig," in *International Gear Conference*, 2014, vol. 2014, pp. 1049–1059.
- [9] A. Mihailidis and I. Nerantzis, "A new system for testing gears under variable torque and speed," *Recent Patents Mech. Eng.*, vol. 2, no. 3, pp. 179–192, 2009.
- [10] J. Huang, H. An, L. Lang, Q. Wei, and H. Ma, "A data-driven multi-scale online joint estimation of states and parameters for electro-hydraulic actuator in legged robot," *IEEE Access*, vol. 8, pp. 36885–36902, 2020.
- [11] Z. Yao, J. Yao, and W. Sun, "Adaptive RISE Control of Hydraulic Systems with

- Multilayer Neural-Networks,” *IEEE Trans. Ind. Electron.*, 2018.
- [12] S. D. Takloo, S. Mozafari, M. Rezazadehmohamadi, and M. Mardani, “Fractional Order PID Control mechanism for Helicopter Gearbox Test Control with internal and External Disturbance,” *Bull. la Société R. des Sci. Liège*.
- [13] A. Maddahi, N. Sepehri, and W. Kinsner, “Fractional-Order Control of Hydraulically Powered Actuators: Controller Design and Experimental Validation,” *IEEE/ASME Trans. Mechatronics*, vol. 24, no. 2, pp. 796–807, 2019.
- [14] M. Li, W. Shi, J. Wei, J. Fang, K. Guo, and Q. Zhang, “Parallel Velocity Control of an Electro-Hydraulic Actuator With Dual Disturbance Observers,” *IEEE Access*, vol. 7, pp. 56631–56641, 2019.
- [15] K. Heybroek and J. Sjöberg, “Model Predictive Control of a Hydraulic Multichamber Actuator: A Feasibility Study,” *IEEE/ASME Trans. Mechatronics*, vol. 23, no. 3, pp. 1393–1403, 2018.
- [16] S. M. Rozali, M. F. Rahmat, N. A. Wahab, and R. Ghazali, “PID controller design for an industrial hydraulic actuator with servo system,” in *2010 IEEE Student Conference on Research and Development (SCORED)*, 2010, pp. 218–223.
- [17] Y. Pan and H. Yu, “Composite learning from adaptive dynamic surface control,” *IEEE Trans. Automat. Contr.*, vol. 61, no. 9, pp. 2603–2609, 2015.
- [18] J. Yang, J. Na, and G. Gao, “Robust model reference adaptive control for transient performance enhancement,” *Int. J. Robust Nonlinear Control*, vol. 30, no. 15, pp. 6207–6228, 2020.
- [19] J. Yang, J. Na, and G. Gao, “Robust adaptive control for unmatched systems with guaranteed parameter estimation convergence,” *Int. J. Adapt. Control Signal Process.*, vol. 33, no. 12, pp. 1868–1884, 2019.
- [20] E. F. Camacho and C. B. Alba, *Model predictive control*. Springer Science & Business Media, 2013.
- [21] V. Balaji and E. Maheswari, “Model Predictive Control Strategy for Industrial Process,” *Bull. Electr. Eng. Informatics*, vol. 1, no. 3, pp. 191–198, 2012.
- [22] T. Alamirew, V. Balaji, and N. Gabbeye, “Comparison of PID Controller with Model Predictive Controller for Milk Pasteurization Process,” *Bull. Electr. Eng. Informatics*, vol. 6, no. 1, pp. 24–35, 2017.
- [23] A. Parvaresh and M. Mardani, “Model predictive control of a hydraulic actuator in torque applying system of a mechanically closed-loop test rig for the helicopter gearbox,” *Aviation*, vol. 23, no. 4, pp. 143–153, 2019.
- [24] D. Wang, D. Zhao, M. Gong, and B. Yang, “Research on robust model predictive control



- for electro-hydraulic servo active suspension systems,” *IEEE Access*, vol. 6, pp. 3231–3240, 2017.
- [25] A. Parvaresh and M. Mardani, “Data-Driven Model-Free Control of Torque-Appling System for a Mechanically Closed-Loop Test Rig Using Neural Networks.,” *Stroj. Vestnik/Journal Mech. Eng.*, vol. 66, no. 5, 2020.
- [26] S. A. Raziei and Z. Jiang, “Dynamic modeling and nonlinear model predictive control of hybrid actuator systems,” in *2017 IEEE National Aerospace and Electronics Conference (NAECON)*, 2017, pp. 119–126.
- [27] K. Pereida and A. P. Schoellig, “Adaptive model predictive control for high-accuracy trajectory tracking in changing conditions,” in *2018 IEEE/RSJ International Conference on Intelligent Robots and Systems (IROS)*, 2018, pp. 7831–7837.
- [28] W.-J. He *et al.*, “Generalized predictive control of temperature on an atomic layer deposition reactor,” *IEEE Trans. Control Syst. Technol.*, vol. 23, no. 6, pp. 2408–2415, 2015.
- [29] Z. Gao, “On the centrality of disturbance rejection in automatic control,” *ISA Trans.*, vol. 53, no. 4, pp. 850–857, 2014.
- [30] J.-S. Kim, “Recent advances in adaptive MPC,” in *ICCAS 2010*, 2010, pp. 218–222.
- [31] T. A. N. Heirung, B. E. Ydstie, and B. Foss, “Dual adaptive model predictive control,” *Automatica*, vol. 80, pp. 340–348, 2017.
- [32] N. Dong, Y. Feng, X. Han, and A. Wu, “An Improved Model-free Adaptive Predictive Control Algorithm For Nonlinear Systems With Large Time Delay,” in *2018 IEEE 7th Data Driven Control and Learning Systems Conference (DDCLS)*, 2018, pp. 60–64.
- [33] Y. Guo, Z. Hou, S. Liu, and S. Jin, “Data-Driven Model-Free Adaptive Predictive Control for a Class of MIMO Nonlinear Discrete-Time Systems With Stability Analysis,” *IEEE Access*, vol. 7, pp. 102852–102866, 2019.
- [34] Z. Wang and J. Wang, “Ultra-local model predictive control: A model-free approach and its application on automated vehicle trajectory tracking,” *Control Eng. Pract.*, vol. 101, p. 104482, 2020.
- [35] D. W. Clarke, “Application of generalized predictive control to industrial processes,” *IEEE Control Syst. Mag.*, vol. 8, no. 2, pp. 49–55, 1988.
- [36] P. Hyatt and M. D. Killpack, “Real-time evolutionary model predictive control using a graphics processing unit,” in *2017 IEEE-RAS 17th International Conference on Humanoid Robotics (Humanoids)*, 2017, pp. 569–576.
- [37] T. Söderström and P. Stoica, “System identification,” 1989.
- [38] N. Ishak, M. Tajjudin, R. Adnan, and H. Ismail, “System identification and model

validation of electro-hydraulic actuator for quarter car system,” *WSEAS Trans. Adv. Eng. Educ*, vol. 4, pp. 27–35, 2017.

[39] L. Ljung, “System identification,” *Wiley Encycl. Electr. Electron. Eng.*, pp. 1–19, 1999.